Nano Research 2016, 9(12): 3924–3936
DOI 10.1007/s12274-016-1261-0
Research Article
ISSN 1998-0124
CN 11-5974/O4

Transparent heaters based on highly stable Cu nanowire films

Haitao Zhai[1,2], Ranran Wang[1] (✉), Xiao Wang[1,2], Yin Cheng[1,2], Liangjing Shi[1], and Jing Sun[1] (✉)

[1] *The State Key Lab of High Performance Ceramics and Superfine Microstructure, Shanghai Institute of Ceramics, Chinese Academy of Sciences, 1295 Dingxi Road, Shanghai 200050, China*
[2] *University of Chinese Academy of Sciences, 19 Yuquan Road, Beijing 100049, China*

Received: 13 July 2016
Revised: 19 August 2016
Accepted: 22 August 2016

KEYWORDS
copper nanowires,
film heater,
transparent conductive film,
anti-oxidation,
flexible device

ABSTRACT

In spite of the recent successful demonstrations of flexible and transparent film heaters, most heaters with high optical transmittance and low applied direct current (DC) voltage are silver nanowire (Ag NW)-based or silver grid-based. In this study, flexible and stretchable copper nanowire (Cu NW)-based transparent film heaters were fabricated through a solution-based process, in which a thin layer of hydrophobic polymers was encapsulated on the Cu NW films. The thin polymer layer protected the films from oxidation under harsh testing conditions, i.e., high temperature, high humidity, and acidic and alkaline environments. The films exhibited remarkable performance, a wide operating temperature range (up to 150 ˚C), and a high heating rate (14 ˚C/s). Defrosting and wearable thermotherapy demonstrations of the Cu NW film heaters were carried out to investigate their practicality. The Cu NW-based film heaters have potential as reliable and low-cost film heaters.

1 Introduction

Transparent film heaters have attracted considerable attention owing to their applicability to a wide range of devices, including wearable devices, outdoor displays, military equipment, and vehicle windows [1–3]. Up to now, tin-doped indium oxide (ITO) has been the most common choice for heating elements because of its excellent optical transmittance and electrical conductivity. Unfortunately, ITO is not a good fit for flexible devices because of its brittleness. Furthermore, indium scarcity and the need for vacuum sputtering also lead to the high cost of ITO. As alternatives to ITO, several transparent and conductive materials such as metal grids [4], carbon nanotubes (CNTs) [5–9], graphene [10, 11], silver nanowires (Ag NWs) [12–18], copper–nickel nanowires (Cu–Ni NWs) [19], and metal nanotroughs [20] have been used as transparent film heaters because of their excellent electrical conductivity. Metal NW film heaters present a fast thermal response even at low applied voltages [12, 14].

Copper is 6% less conductive than silver but 1,000 times more abundant and 100 times less expensive [21]. Thus, replacing Ag NWs with copper NWs should

Address correspondence to Jing Sun, jingsun@mail.sic.ac.cn; Ranran Wang, wangranran@mail.sic.ac.cn

offer comparable levels of performance at a lower cost. Cu NW films are among the most promising candidates as low-cost and low-applied voltage film heaters because of their flexibility, high transparency, excellent electrical conductivity, and solution-based fabrication process [22–24]. However, few reports related to Cu NW-based film heaters have been found. Notwithstanding their excellent optical and electrical performance, Cu NW films have some inherent drawbacks as compared to Ag NWs, including (1) the need for complicated post-treatment techniques to obtain outstanding electrical conductivity and (2) their inferior anti-oxidation stability, especially when exposed to harsh environments such as increased temperature, humidity, or acidity. The second issue is particularly critical because film heaters are expected to endure such hostile conditions.

To overcome these problems, Cu–Ni NWs [19, 21, 25, 26], Cu–Ag NWs [25, 27], and Cu–Zn and Cu–Sn NWs [28] have been synthesized in the past. However, these bimetal nanowires do not fully satisfy the requirements of anti-oxidation, and most of them exhibit poor optical and electrical performance as compared to Cu NWs. Deng et al. [29], Ahn et al. [30], and Shi et al. [31] have encapsulated nanowire networks with graphene and improved the anti-oxidation properties of Cu NWs, but the growth of graphene by chemical vapor deposition (CVD) and its transfer have increased the complexity of the process and the total cost. In this study, transparent electrodes with superb optical and electrical performance were fabricated on various substrates with home-made ultralong Cu NWs through a solution-based process. Hydrophobic polymers, including poly(methyl methacrylate) (PMMA), polyacrylate (PA), and polydimethylsiloxane (PDMS), have been proven effective in protecting Cu NWs from oxidation under harsh testing conditions such as high temperature, high humidity, and acidic and alkaline environments. Thus, the oxidation process of Cu NWs under different conditions and the anti-oxidation mechanism are also elucidated. Flexible and stretchable Cu NW film heaters with a wide operating temperature range (up to 150 ℃) and high heating rate (14 ℃/s), values that are comparable to those of CuZr metallic glass (MG) nanotroughs (120 ℃ with 5 V direct current (DC) bias) [20] and even superior to those of Ag NW films (120 ℃ with 7 V DC bias) [32], were investigated for the first time. Defrosting and wearable thermotherapy demonstrations based on the Cu NW film heaters were carried out to investigate their practicality. We believe that the superb heating and mechanical performance, and low cost, together with the convenient fabrication process of Cu NW–polymer film heaters open up great opportunities for large-scale electronics applications in the future.

2 Experimental

2.1 Preparation of Cu NWs

For the Cu NW synthesis, we used the modified self-catalytic method that was previously reported by our research team [22, 24]. In a typical synthesis, 10 mL of oleylamine (OA) and 0.5 g of cetrimonium bromide (CTAB) were dissolved in a glass vial at 180 ℃. Then, 200 mg of copper acetylacetonate ($Cu(acac)_2$) was added and mixed evenly. After that, 5–7 μL of a Pt nanoparticle suspension was added as a catalyst. The Pt nanoparticles were synthesized as follows: 2 mg of platinous chloride was dispersed into 1.2 mL of ethylene glycol, then added to 2.3 mL of ethylene glycol and kept at 160 ℃ for 90 s. The mixtures were then kept at 180 ℃ for 12 h, resulting in the formation of reddish cotton-like sheets that settled at the bottom. After rinsing with toluene and isopropanol several times, the nanowires were stored in isopropanol.

2.2 Preparation of Cu NW transparent conductive film

Typically, Cu NWs were dispersed in isopropanol by bath sonication for 1–2 min and then sprayed onto the substrate. Glass slides (1.1 mm in thickness) and polyethylene terephthalate (PET) films (0.1 mm in thickness) were used as substrates and pretreated with O_2 plasma for 60 s to obtain a homogeneous surface before spraying. Finally, the films were treated with H_2 plasma to remove the oxidized layers and the resident OA on the surfaces of the Cu NWs.

2.3 Fabrication and characterization of Cu NW-based heaters

PMMA was dissolved in 1,2-dichlorobenzene with a concentration of 46 mg/mL and spin coated onto the

Cu NW transparent conductive films. The thickness of the PMMA was controlled by the velocity of rotation (1,000–5,000 rpm). The as-prepared samples are denoted as Cu NW-1000, Cu NW-3000, and Cu NW-5000, which refer to the corresponding velocity of rotation of the spin coating. The Cu NW-based film heaters were fabricated using a two-terminal side-contact configuration. The DC voltage was supplied by an electrochemical workstation (CHI 660D, CH) to the film heaters through the copper contacts at the film edge. Silver paste (SCP003, ELECTROLUBE) and Cu foil conductive tape (3M) were used to decrease the contact resistance between the Cu NW-based transparent conductive films and the external connection. The temperature of the films was measured using an IR thermal imager (SC305, FLIR). For the defrost test, a Cu NW/PMMA composite film with a surface resistivity of 17 Ω/sq was prepared and attached to the glass substrate. The film was placed in a refrigerator for 30 min to induce frost formation, after which an input voltage of 5 V was applied to the film heater.

2.4 Characterization of samples

The morphology of the samples was characterized by field-emission scanning electron microscopy (FESEM, Magellan 400, FEI, USA). The transmittance data were collected using a Lambda-950 UV-Vis spectrophotometer (PerkinElmer, Waltham, MA, USA). The transmittance data did not include the contribution from the substrates. The substrate contribution was deducted in order to obtain a more accurate comparison of the samples with different substrates and from other reported works. Surface-resistivity measurements were carried out using a standard four-point probe method using a Loresta-EP MCP-T 360 instrument. The aging tests were carried out in a constant temperature and humidity test chamber (Espec Corp SH-222). During the aging tests, we used temperature and relative humidity (RH) conditions of 80 ℃–20% (RH), 25 ℃–70% (RH), and 80 ℃–100% (RH). The temperature responses of the film heaters were recorded using an infrared (IR) camera (SC305, FLIR). The bending tests were carried out with a movable-stage apparatus (ZXT_050-300_MA06, Shanghai Zhengxin Opto-Electrical Technology Co. Ltd., China). The resistance variation of the heaters was investigated by measuring the resistance of the copper contacts at the two terminals with a multimeter during the bending tests (10,000 cycles). The bending rate was one cycle per 2 s (0.5 Hz).

3 Results and discussion

Cu NWs with diameters of 60–80 nm and lengths of more than 50 μm were prepared by the modified method reported in our previous work [22, 24]. The synthesis details can be found in the Experimental section. Figure 1(a) schematically illustrates the fabrication process of the conductive, transparent Cu NW films. The substrate was first treated by O_2 plasma to remove any residual greasy dirt. Subsequently, the Cu NW dispersion in isopropanol was sprayed onto the substrate. In order to enhance the conductivity of the Cu NWs films, H_2 plasma was used to remove the oxidized layers and the resident OA on the surface of Cu NWs. Negligible change in the sheet resistance and optical transmittance over the range of 400–800 nm was observed after coating the PMMA layer (Fig. 1(d)) because of the excellent transparency of PMMA. As shown in Fig. 1(e), the Cu NW thin films showed high optical–electrical performance of 17 Ω/sq at 84% transparency (T) and 96 Ω/sq at 91% T, which is equivalent to many Ag NW-based thin films and superior to most graphene- and CNT-based thin films. The superb performance is attributed to the high aspect ratio of the Cu NWs and the enhanced interfacial contact between nanowires resulting from the H_2 plasma treatment [33], as shown in Fig. 1(f). Cu NW films with such high performance are expected to be good candidates for transparent heaters. Unfortunately, nanowires are easily detached from substrates due to weak adhesion. Cu NWs are also prone to oxidation at high temperatures, which will hinder their use as film heaters. To conquer these issues, a thin layer of highly transparent hydrophobic polymers, which can hinder the permeation of air and aqueous molecules, was spin coated onto the Cu NW films as a protective layer. PMMA, PA, and silicon rubber (PDMS and Ecoflex®) were investigated as the protective layers. The PMMA layer is discussed in detail here as an example. As shown in Fig. 1(g), a thin layer PMMA covered the top of the Cu NW network homogeneously,

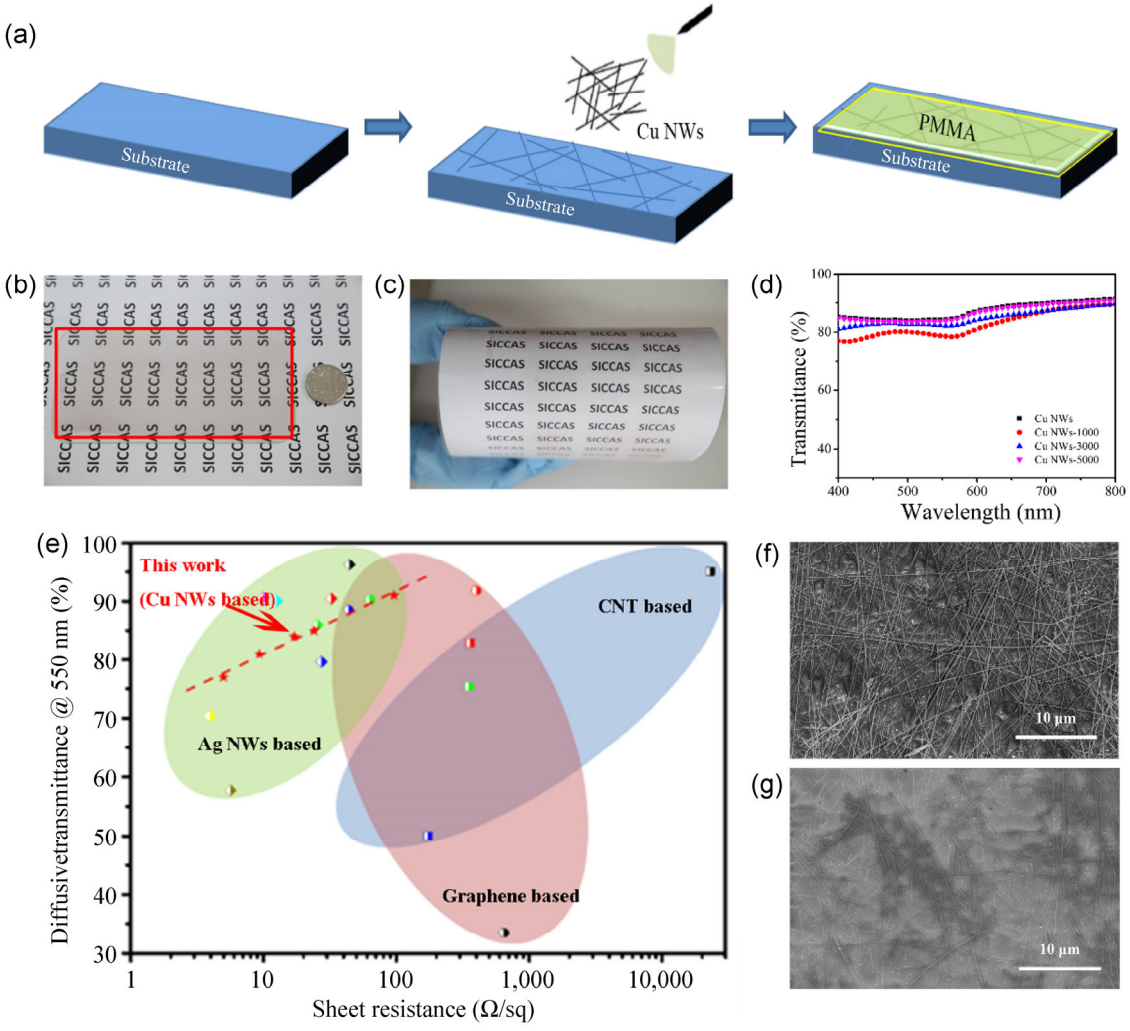

Figure 1 (a) Schematic of Cu NW film preparation. Photographs of Cu NW film (b) on glass and (c) on PET. (d) Transmission of the Cu NW and Cu NW/PMMA composite films in the wavelength range of 400–800 nm. (e) Plot of transmittance versus sheet resistance for Cu NWs and other heating systems from the literature. FESEM images of (f) Cu NWs and (g) Cu NW/PMMA film.

leaving the nanowires embedded but still visible. With the thin protective layer, the adhesion of the nanowires on the substrates was enhanced, as confirmed by the tape test (Fig. S1 in the Electronic Supplementary Material (ESM)). None of the nanowires were detached from the substrate for the Cu NW/PMMA composite electrode, even after 100 tape tests, whereas the pristine Cu NW network was easily detached.

The stability of the Cu NW films with and without the PMMA protective layers was investigated systematically under different aging conditions. Here, we use the normalized change in the sheet resistance, $\Delta R/R_0$, where R_0 is the initial sheet resistance and ΔR is the change in sheet resistance with time, versus time as an estimate of stability. The time it took for $\Delta R/R_0$ to double was used as the evaluation criterion; a longer time indicated higher stability [25]. Films with the same starting sheet resistance were chosen as the test samples to avoid the influence of nanowire density. As seen in Fig. 2(a), after aging under ambient temperature and humidity (approximately 25 ˚C, 40%–50% RH) for 1 month, the sheet resistance of the Cu NW films increased slightly, whereas those of the Cu NW/PMMA composite films remained completely stable, which proved the protective effect of the PMMA layers. When we elevated the aging temperature to 80 ˚C while keeping the humidity as low as 20%, the pristine Cu NW films lost their conductance quickly

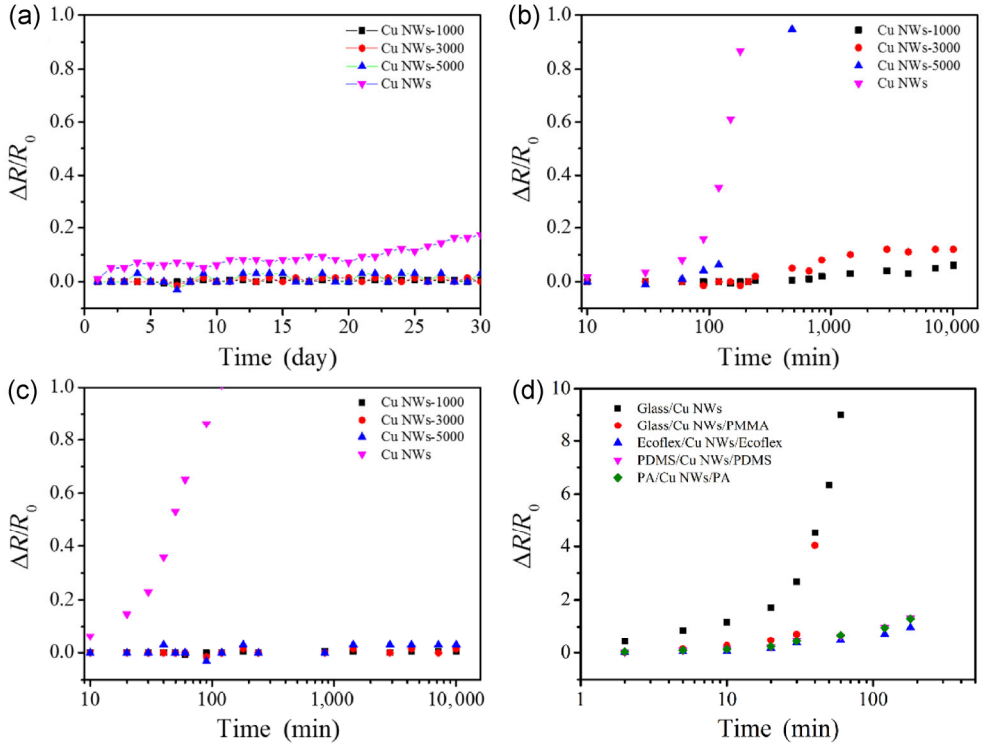

Figure 2 Plots of sheet resistance versus time for transparent conductive films of Cu NWs under different temperatures and humidity conditions: (a) room temperature, (b) 80 ℃–20% (RH), (c) 25 ℃–70% (RH), and (d) 80 ℃–100% (RH).

due to the accelerated oxidation kinetics. The Cu NW-5000 film (coated with PMMA at a rotation rate of 5,000 rpm) exhibited enhanced stability. However, it still lost its conductance within 1,000 min. By comparison, the Cu NW-3000 and Cu NW-1000 films showed remarkable stability up to 10,000 min at 80 ℃–20% RH (Fig. 2(b)). The results demonstrated that a suitable thickness of the PMMA layer is of great concern to the effective protection of Cu NWs at elevated temperatures considering the different thermal expansivities of copper and PMMA.

In addition to temperature, humidity is another important factor that influences the oxidation process of metal nanowires. When the relative humidity was elevated to 70% at 25 ℃, the pristine Cu NW films oxidized rapidly because they reacted with CO_2 and H_2O molecules [25, 31]. The PMMA layers prevented the permeation of such reactive molecules and provided remarkable stability up to 10,000 min, as shown in Fig. 2(c). At high temperature and high humidity (80 ℃–100% RH), the pristine Cu NW films oxidized within several minutes. Coating with the PMMA layer could improve the stability at the start of aging; however, it would accelerate the oxidation after that. The reason for these contrary effects is thought to be that the PMMA layer prevents the permeation of O_2 and water vapor in the beginning. However, because of the mismatched thermal expansion between the substrate and the protection layer, small cracks might appear and gather water droplets, which could make up a primary battery and accelerate the oxidation of the Cu NWs. Much better protective performance has been obtained for the same substrate and protection layer, such as Ecoflex®/Cu NW/Ecoflex®, PDMS/Cu NW/PDMS, and PA/Cu NW/PA.

In order to further understand the oxidation of Cu NWs with and without PMMA protection under different temperature and humidity conditions, the morphology of the Cu NWs after aging tests was characterized. As shown in Fig. 3, no obvious changes in the morphology of the Cu NWs with PMMA protection were observed after aging at room temperature for 1 month, at 80 ℃–20% (RH) for 1,000 min, and at 25 ℃–70% (RH) for 1,000 min (Figs. 3(a), 3(c),

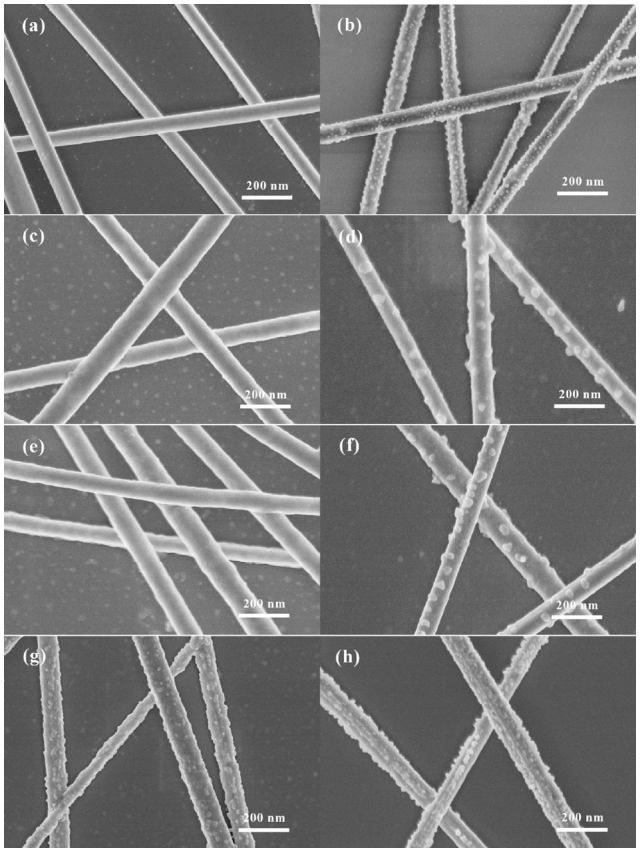

Figure 3 FESEM images of Cu NWs after environmental tolerance tests under different temperature and humidity conditions: at room temperature for 1 month (a) with and (b) without the protection of PMMA; at 80 ℃–20% (RH) for 1,000 min (c) with and (d) without the protection of PMMA; at 25 ℃–70% (RH) for 1,000 min (e) with and (f) without the protection of PMMA; and at 80 ℃–100% (RH) for 60 min (g) with and (h) without the protection of PMMA.

and 3(e), respectively). However, a large number of small nanoparticles agglomerated on the uncovered Cu NWs after aging at room temperature for 1 month (Fig. 3(b)), and larger and sparser nanoparticles were found on the Cu NWs after aging at 80 ℃–20% (RH) for 1,000 min and at 25 ℃–70% (RH) for 1,000 min (Figs. 3(d) and 3(f), respectively). It was confirmed in our previous research that the nanoparticles on the Cu NWs were non-electrical conductive oxides of copper [31]. The oxide nanoparticles, especially the larger ones, therefore hindered the electron transport between inter-nanowires, which explains the sharp increase of the sheet resistance. As for Cu NWs after aging at 80 ℃–100% (RH) for 60 min, a greater number of large nanoparticles and even cracks were observed, which explains the tremendous resistance variation of the films.

Raman and X-ray photoelectron spectroscopy (XPS) spectra were used to characterize the element changes of the Cu NWs after the environmental tests. As shown in Fig. 4, no peaks for the oxides of copper were observed in the spectra of the Cu NW/PMMA composite film samples after aging under the conditions of room temperature, elevated humidity, and elevated temperature, verifying the anti-oxidation effect of the PMMA layer. By comparison, strong peaks of oxides of copper appeared in the uncovered Cu NW film samples. Interestingly, the Cu NW/PMMA composite film tended to form cuprous oxide (Cu(I)) under the condition of elevated temperature and very low relative humidity, whereas copper oxide (Cu(II)) was mainly formed under the condition of high humidity. This is reasonable because cuprous oxide is thermodynamically stable and the Cu NWs would be oxidized to Cu_2O first [31], although Cu_2O is not chemically stable and can be further oxidized under watery environments. The Cu 2p3/2 XPS analysis of the Cu NW film samples after the environmental tolerance tests affirmed the results of the Raman characterization. The XPS peaks of Cu(0) (932.2–932.7 eV) and Cu(I) (932.0–932.6 eV) have an overlapping Cu 2p3/2 binding energy (BE) range, and so it is improper to distinguish between Cu and Cu_2O by the XPS spectra of Cu 2p3/2. However, Cu(II) species have a significant peak shift. Figure 5 shows the spectrum of the Cu NW with and without PMMA protection at 25 ℃–70% (RH) and at 80 ℃–20% (RH) for 1,000 min. The peak at ~932.8 eV was assigned to the overlap of Cu and Cu_2O, the peak at ~933.8 eV was assigned to CuO, and the peak at ~934.7 eV was assigned to $Cu(OH)_2$. As seen in the figure, the strong peak of CuO appeared in the unprotected Cu NW film aged at 25 ℃–70% (RH), which is consistent with the Raman analysis. In addition, the peak of $Cu(OH)_2$ was detected, proving the reaction of Cu_2O with water under high humidity conditions. CuO was detected in all the Cu NW film samples, which is distinct with the Raman analysis. The detection limit should be responsible for the difference.

Furthermore, the Cu NW/PMMA composite electrodes endured 6 wt.% HCl and 10 wt.% NaOH solution for 0.5 h, which is the testing standard for

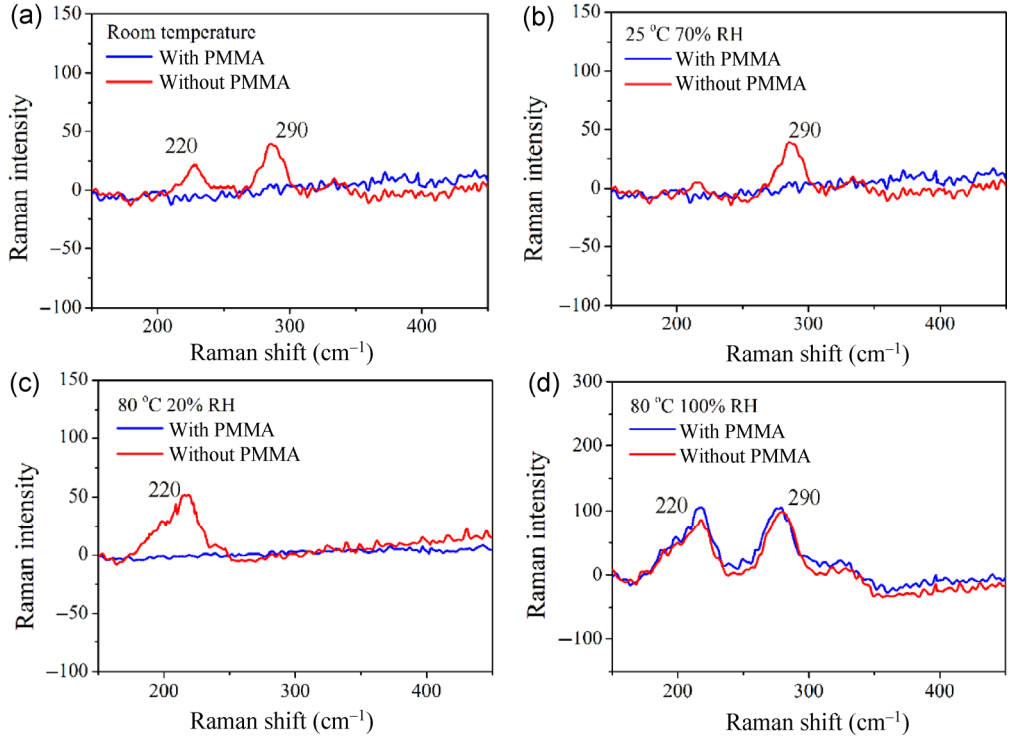

Figure 4 Raman spectra of Cu NWs after the environmental tolerance test under different temperature and humidity conditions: (a) at room temperature for 1 month with and without the protection of PMMA; (b) at 80 ˚C–20% (RH) for 1,000 min with and without the protection of PMMA; (c) at 25 ˚C–70% (RH) for 1,000 min with and without the protection of PMMA; and (d) at 80 ˚C–100% (RH) for 60 min with and without the protection of PMMA.

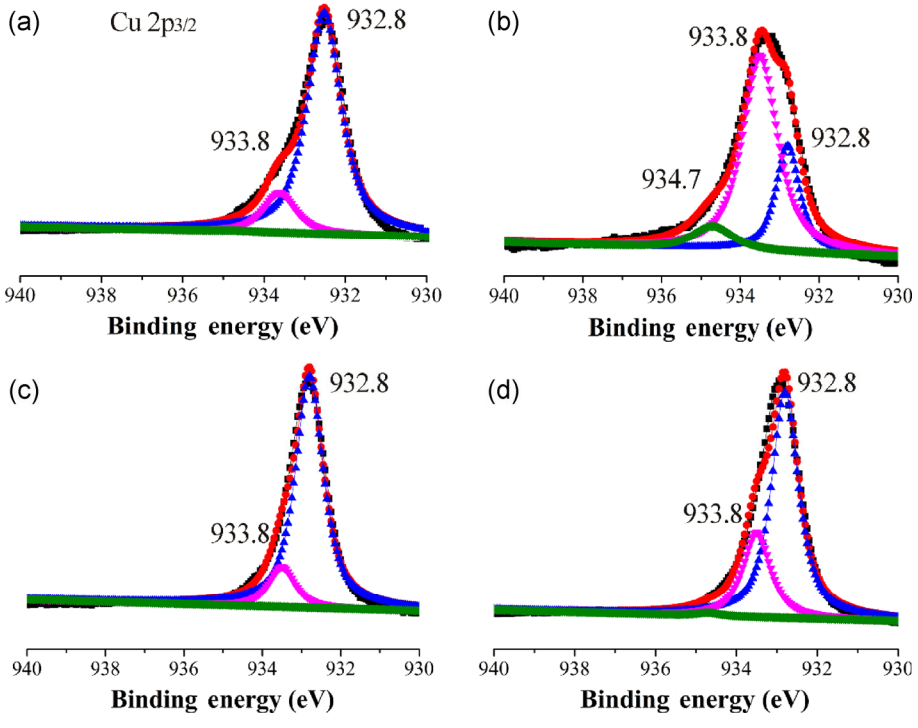

Figure 5 Cu 2p3/2 XPS spectrum of Cu NWs after the environmental tolerance test under different temperature and humidity conditions: at 25 ˚C–70% (RH) for 1,000 min (a) with and (b) without the protection of PMMA; and at 80 ˚C–20% (RH) for 1,000 min (c) with and (d) without the protection of PMMA.

commercial ITO. The stability of the Cu NWs might be the biggest obstacle in terms of storage and work-piece processing. The excellent anti-thermal oxidation ability and the anti-moisture corrosion function of the PMMA layer were very effective in enhancing the weatherability and acid–alkali resistance of the Cu NWs electrodes. It must be pointed out that the PMMA layer can be conveniently removed by acetone without any damage to the Cu NWs if a clean Cu NW surface is needed. In addition to PMMA, the protective layer can be broadened to many other polymer molecules. Thus, PDMS, Ecoflex®, and PA were also examined, and they exhibited effectiveness in terms of protecting the Cu NWs from oxidation.

Cu NW transparent electrodes have potential to be used as flexible invisible heaters due to their high optical–electrical performance. To evaluate their heating performance, transparent Cu NW electrodes coated on glass or PET substrates were tested under constant DC bias of 1.5–10 V with copper conductive tape as the contact electrode. Figures 6(a)–6(c) show the time-dependent temperature curves of the Cu NW films on glass slides with sheet resistances of 6.1, 17, and 90 Ω/sq, respectively. The temperature responses of the heating films were recorded using an infrared camera (SC305, FLIR). The curves show that the surface temperature of the films increases by applying constant DC bias until reaching the saturation point. Figure 6(d) shows that the saturation temperature of the heating film is proportional to the square of the input voltage. This is because the rate of thermal energy generation via Joule heating equals the rate of thermal energy loss at quasi-static thermal equilibrium and the thermal energy generation via Joule heating is proportional to the square of the input voltage [34]. In addition, the lower the sheet resistances (RS), the higher the saturation temperature with the same input voltage. Because the Cu NW films exhibited low sheet resistance, high saturation temperatures were expected. Unfortunately, the uncovered Cu NWs films failed quickly because

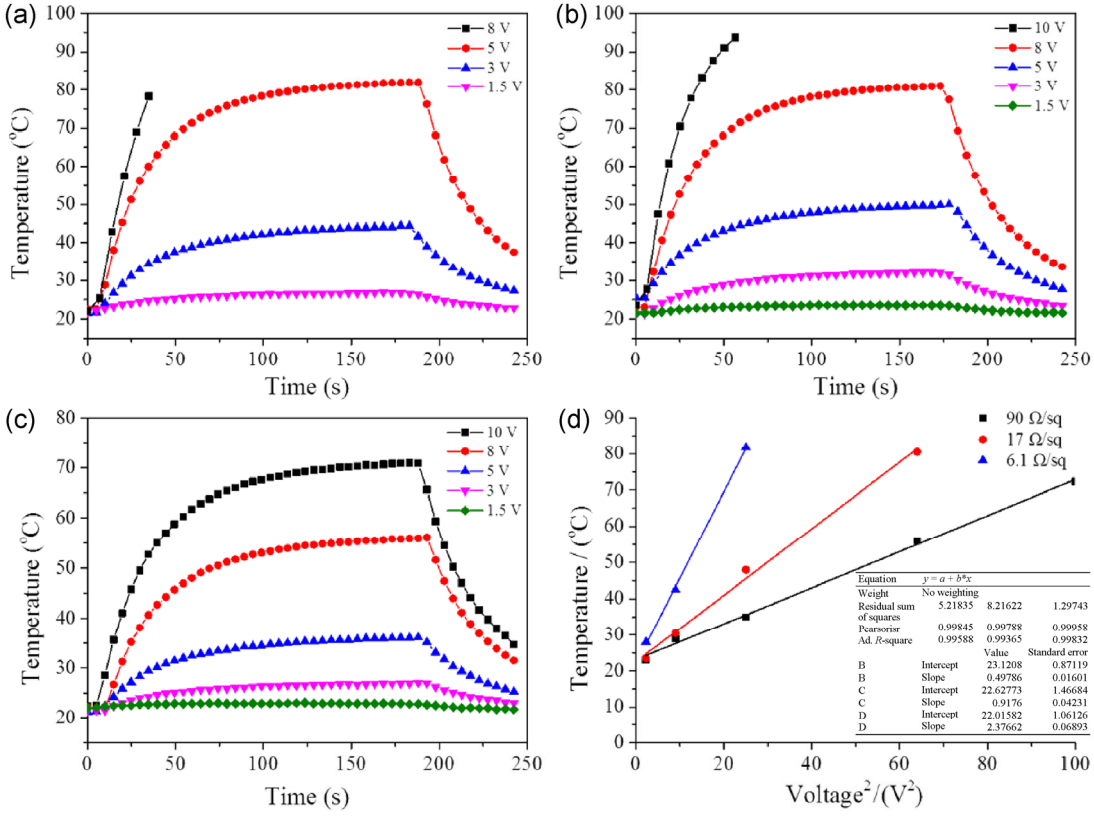

Figure 6 Time-dependent temperature curves of the Cu NW films on glass plates with sheet resistances of (a) 6.1, (b) 17, and (c) 90 Ω/sq at input voltages of 1.5–10 V under ambient conditions. (d) The saturation temperature of the three Cu NW films versus the square of the input voltage.

of oxidation when the temperature was above 85 ℃.

After coating the Cu NWs with a thin layer of PMMA, the stability of the Cu NW films was greatly enhanced, as discussed above. Temperatures as high as 150 ℃ were reached within 70 s, as shown in Fig. 7(a). This performance is superior to that of CNT- or graphene-based film heaters, which have high sheet resistance (349 Ω/sq at 72% T and 80 ℃ with 40 V DC bias) [7]. In other words, the Cu NW-based heating film requires a lower voltage to obtain the desired temperature as compared to other types of heaters, implying the low power consumption of this heater.

Rapid heating and high saturation temperatures indicate the application of Cu NW-based heating films as defrosters. To evaluate the defrosting performance, a Cu NW/PMMA composite film on a glass substrate was put in a refrigerator for 30 min to allow frost to develop [35]. With the application of a DC bias of 5 V on the film heater, the frost on the surface was completely removed within 60 s. The symbols in the background became clearly visible, as exhibited in Figs. 7(c) and 7(d) and in Movie S1 (in the ESM). The fast defrosting at low voltages, together with the solution based fabrication process, enables the Cu NW composite films to be used as inexpensive heating coatings in many electrical appliances.

In order to lead the way in flexible film heaters, Cu NW/PMMA composite films on PET substrates were fabricated. Figures 8(a)–8(c) show the time-dependent temperature curves of the Cu NW/PMMA composite films with PMMA spin-coating speeds from 1,000 to 5,000 rpm. Figure 8(d) shows the saturation temperature and heating rate of the three Cu NW films versus the input voltage. A higher saturation temperature and heating rate were obtained when the protective layer was thinner under the same voltage, which could be because of the lower heat capacity according to the following equation

$$C_p \times m \times \Delta T = \frac{U^2 \times t}{R}$$

At quasi-static thermal equilibrium, the rate of thermal energy loss is equal to the rate of thermal energy generation via Joule heating [34]. For each film, the saturation temperature and the time required to reach a

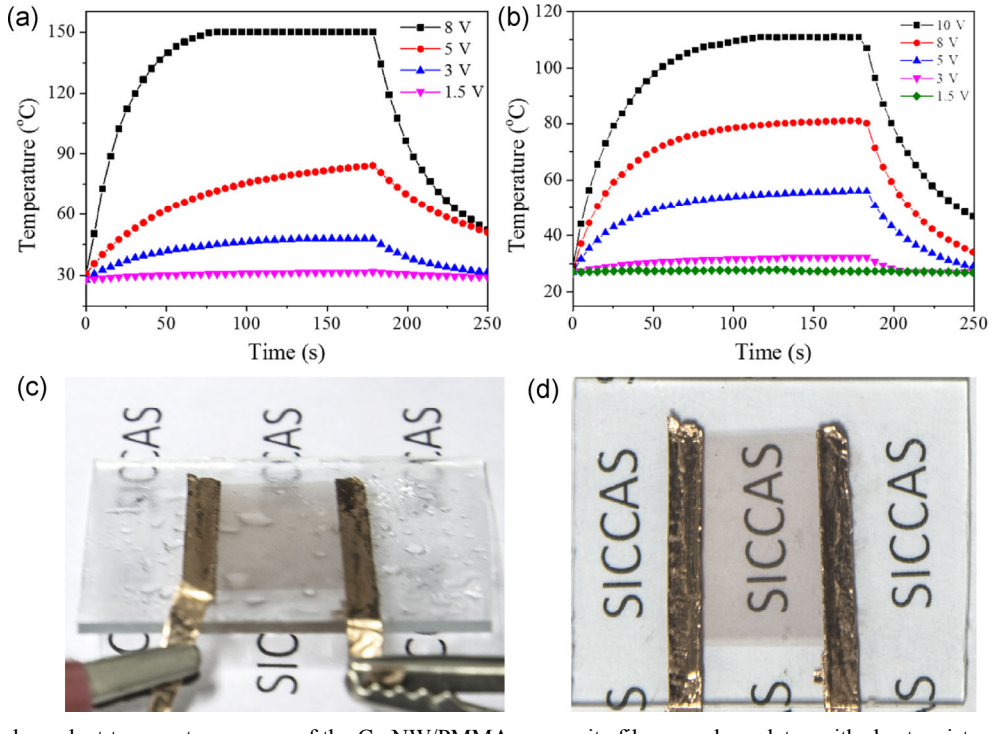

Figure 7 Time-dependent temperature curves of the Cu NW/PMMA composite films on glass plates with sheet resistances of (a) 6.1 and (b) 17 Ω/sq at input voltages of 1.5–10 V under ambient conditions. Defrosting test results of a Cu NW/PMMA composite film heater (c) before and (d) after defrosting.

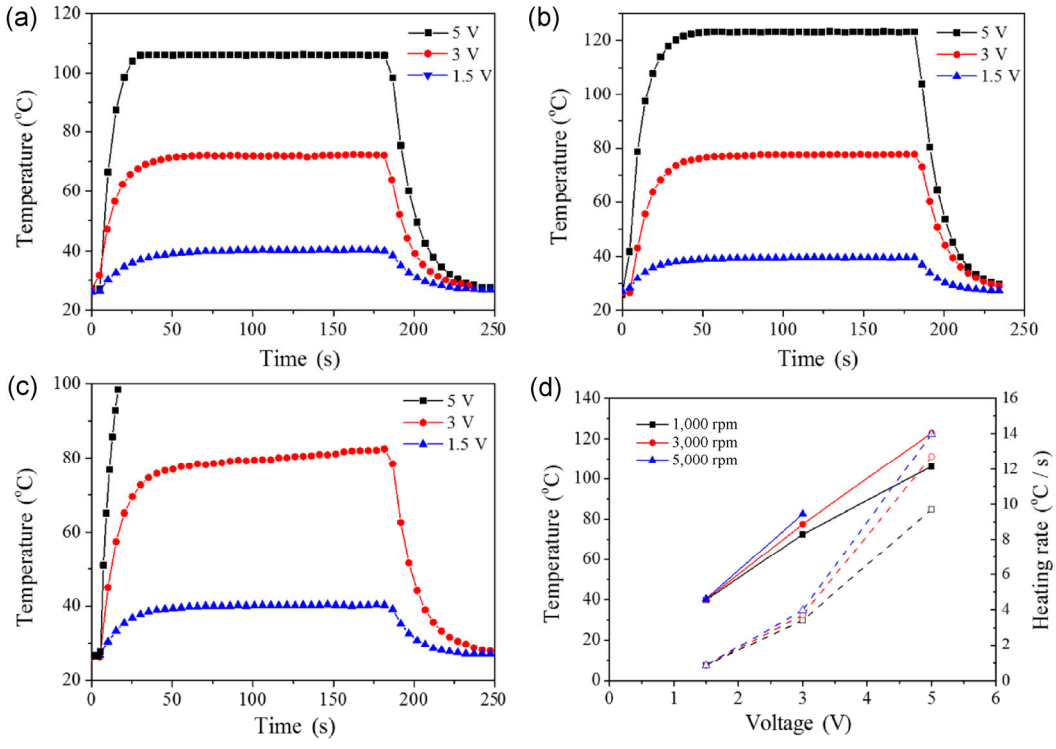

Figure 8 Time-dependent temperature curves of (a) Cu NW-1000, (b) Cu NW-3000, and (c) Cu NW-5000 on PET films at input voltages of 1.5–5 V under ambient conditions. (d) The saturation temperature and heating rate of the three Cu NW films versus the input voltage.

given temperature should be proportional to the heat capacity due to the steady thermal energy generation via Joule heating with a given input voltage. For the same reason, films on PET substrates (0.1 mm thick) achieved higher saturation temperatures and heating rates with the same input voltage and sheet resistance as compared to films on glass slides (1.1 mm thick). The Cu NW-3000-PET composite film achieved a temperature of 120 ℃ under a voltage of 5 V within 30 s. The heating rate was high as 14 ℃/s, which is comparable to that of CuZr MG nanotroughs (120 ℃ with 5 V DC bias) [20] and even superior to that of Ag NW films (120 ℃ with 7 V DC bias) recently reported [32]. To further improve the performance at high temperature, protection polymers with better performance (such as those with oxygen and water–vapor barrier properties, thermostability, and combined stability with the substrates at high temperature and high humidity) should be chosen. In addition, it was found that the protection layer might detach from the NWs and the substrates under high temperature and high humidity conditions because of the mismatched thermal expansion. Therefore, optimizing the interface combination is another route to further improving the thermal stability of Cu NW-based heaters. Moreover, alloying and covering Cu NWs with inorganic protecting layers such as AlO_3, ZnO, TiO_2, etc., can also improve the high-temperature performance.

The mechanical flexibility and durability of the Cu NW/PMMA composite film heaters were investigated via measuring the resistance change during bending tests (10,000 cycles), as shown in Fig. 9. The bending rate was one cycle per 2 s (0.5 Hz) and the bending radius was 3 mm. The initial sheet resistances of the Cu NW/PMMA composite and PET/ITO film heaters were 17 and 15 Ω/sq, respectively. The resistance variation of the PET/ITO film heater increased to hundreds of thousands times after 10,000 bending cycles. Especially when bending outward (ITO or Cu NWs on the outer flank), the resistances doubled after 20 bending cycles. In contrast, we observed little resistance variation (<10%) of the Cu NW/PMMA composite film heater after 10,000 bending cycles, which demonstrates their applicability to curved devices. Moreover, a highly stretchable Ecoflex®/Cu NW/Ecoflex® film heater was fabricated, as shown in

Movie S2 (in the ESM), which presents the potential applications in wearable electronics and thermotherapy [20, 32, 36]. Briefly, the Cu NW film on a glass slide was transferred onto a pre-polymerized and pre-stretched Ecoflex® substrate, followed by post-treatment for 30 min at 80 ˚C in an oven. After peeling off the glass slide, a thin layer of Ecoflex® was coated onto the surface of the Cu NW film to enhance its stability. Ecoflex® was chosen as the protective layer because it is highly stretchable, whereas a PMMA layer is destroyed through stretching. After releasing the Ecoflex® substrate, a stretchable Cu NW film was obtained. As shown in Fig. 9(c), the heater was stretched up to 80% while maintaining the DC bias (1.5 V). This stretching did not change the temperature significantly. The Cu NW-based stretchable heater can be applied in portable thermotherapy devices because of its low working voltage. Figure 9(d) presents a photograph and an IR image of a skin-attached heater, which can elevate the temperature up to 50 ˚C with 3 V DC bias.

4 Conclusions

In this work, transparent electrodes with superb optical–electrical performance (17 Ω/sq at 84% *T* and 96 Ω/sq at 91% *T*) on various substrates were fabricated with ultra-long Cu NWs through a solution-based process. Hydrophobic polymers, including PMMA, PA, and PDMS, were proven effective in protecting the Cu NWs from oxidation under harsh testing conditions, such as high temperature, high humidity, and acidic and alkaline environments. The polymer protection layer can prevent the permeation of reactive molecules and provide the Cu NWs with remarkable stability. Defrosting and wearable thermotherapy demonstrations based on Cu NW film heaters were carried out to investigate their practicability. Flexible and stretchable Cu NW film heaters with a wide operating temperature range (up to 150 ˚C) and high heating rate (14 ˚C/s) were investigated. The Cu NW-based film heaters have potential applications as reliable and low-cost film heaters.

Acknowledgements

This work was financially supported by the National Basic Research Program of China (No. 2012CB932303), the National Natural Science Foundation of China (No. 61301036), Shanghai Municipal Natural Science Foundation (Nos. 13ZR1463600 and 13XD1403900),

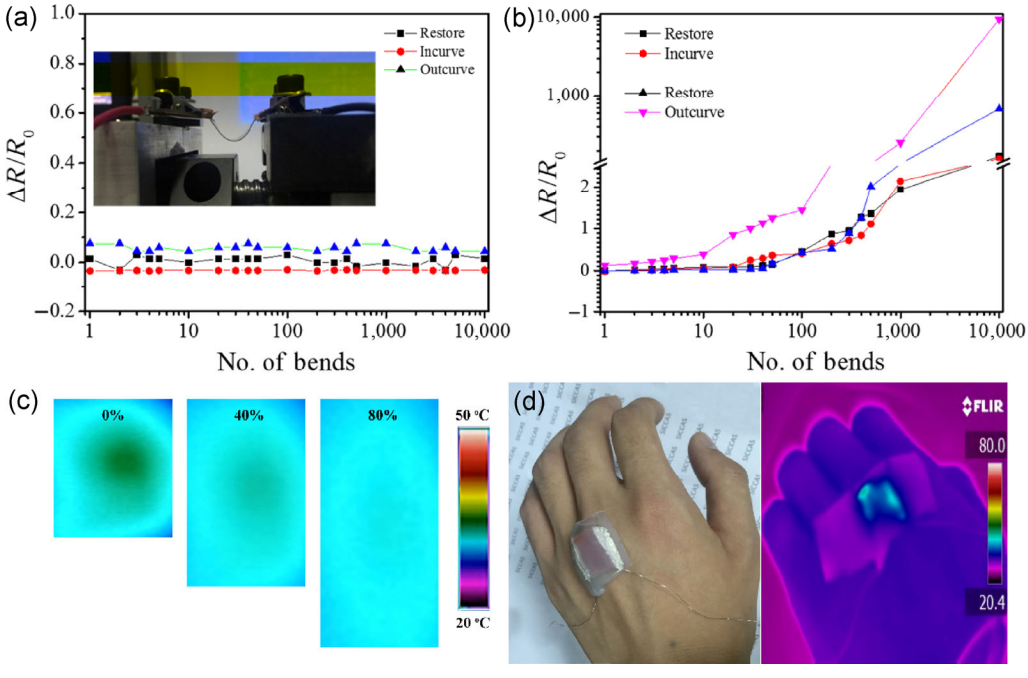

Figure 9 Variations in the resistance of (a) PET/Cu NW/PMMA composite films and (b) PET/ITO transparent heaters during 10,000 cycles of bending tests. (c) Infrared photograph and (d) application examples of Cu NW-based stretchable heater.

Youth Innovation Promotion Association CAS (No. 2014226), and the Shanghai Key Basic Research Project (No. 16JC1402300).

Electronic Supplementary Material: Supplementary material (further details of the tap test of Cu NWs based film, the defrosting and the wearable thermotherapy demonstrations) is available in the online version of this article at http://dx.doi.org/10.1007/s12274-016-1261-0.

References

[1] Sorel, S.; Bellet, D.; Coleman, J. N. Relationship between material properties and transparent heater performance for both bulk-like and percolative nanostructured networks. *ACS Nano* **2014**, *8*, 4805–4814.

[2] Hecht, D. S.; Hu, L. B.; Irvin, G. Emerging transparent electrodes based on thin films of carbon nanotubes, graphene, and metallic nanostructures. *Adv. Mater.* **2011**, *23*, 1482–1513.

[3] Bae, J. J.; Lim, S. C.; Han, G. H.; Jo, Y. W.; Doung, D. L.; Kim, E. S.; Chae, S. J.; Huy, T. Q.; Van Luan, N.; Lee, Y. H. Heat dissipation of transparent graphene defoggers. *Adv. Funct. Mater.* **2012**, *22*, 4819–4826.

[4] Jang, Y.; Kim, J.; Byun, D. Invisible metal-grid transparent electrode prepared by electrohydrodynamic (EHD) jet printing. *J. Phys. D: Appl. Phys.* **2013**, *46*, 155103.

[5] Yoon, Y. H.; Song, J.-W.; Kim, D.; Kim, J.; Park, J.-K.; Oh, S.-K.; Han, C.-S. Transparent film heater using single-walled carbon nanotubes. *Adv. Mater.* **2007**, *19*, 4284–4287.

[6] Kang, T. J.; Kim, T.; Seo, S. M.; Park, Y. J.; Kim, Y. H. Thickness-dependent thermal resistance of a transparent glass heater with a single-walled carbon nanotube coating. *Carbon* **2011**, *49*, 1087–1093.

[7] Jang, H.-S.; Jeon, S. K.; Nahm, S. H. The manufacture of a transparent film heater by spinning multi-walled carbon nanotubes. *Carbon* **2011**, *49*, 111–116.

[8] Jung, D.; Kim, D.; Lee, K. H.; Overzet, L. J.; Lee, G. S. Transparent film heaters using multi-walled carbon nanotube sheets. *Sensor. Actuat. A: Phys.* **2013**, *199*, 176–180.

[9] Liu, P.; Zhou, D. L.; Wei, Y.; Jiang, K. L.; Wang, J. P.; Zhang, L.; Li, Q. Q.; Fan, S. S. Load characteristics of a suspended carbon nanotube film heater and the fabrication of a fast-response thermochromic display prototype. *ACS Nano* **2015**, *9*, 3753–3759.

[10] Sui, D.; Huang, Y.; Huang, L.; Liang, J. J.; Ma, Y. F.; Chen, Y. S. Flexible and transparent electrothermal film heaters based on graphene materials. *Small* **2011**, *7*, 3186–3192.

[11] Kang, J. M.; Kim, H.; Kim, K. S.; Lee, S.-K.; Bae, S. K.; Ahn, J.-H.; Kim, Y.-J.; Choi, J.-B.; Hong, B. H. High-performance graphene-based transparent flexible heaters. *Nano Lett.* **2011**, *11*, 5154–5158.

[12] Cheong, H.-G.; Song, D.-W.; Park, J.-W. Transparent film heaters with highly enhanced thermal efficiency using silver nanowires and metal/metal-oxide blankets. *Microelectron. Eng.* **2015**, *146*, 11–18.

[13] Li, J. P.; Liang, J. J.; Jian, X.; Hu, W.; Li, J.; Pei, Q. B. A flexible and transparent thin film heater based on a silver nanowire/heat-resistant polymer composite. *Macromol. Mater. Eng.* **2014**, *299*, 1403–1409.

[14] Huang, Q. J.; Shen, W. F.; Fang, X. Z.; Chen, G. F.; Guo, J. C.; Xu, W.; Tan, R. Q.; Song, W. J. Highly flexible and transparent film heaters based on polyimide films embedded with silver nanowires. *RSC Adv.* **2015**, *5*, 45836–45842.

[15] Woo, J. S.; Han, J. T.; Jung, S.; Jang, J. I.; Kim, H. Y.; Jeong, H. J.; Jeong, S. Y.; Baeg, K. J.; Lee, G. W. Electrically robust metal nanowire network formation by *in-situ* interconnection with single-walled carbon nanotubes. *Sci. Rep.* **2014**, *4*, 4804.

[16] Kim, A. Y.; Kim, M. K.; Hudaya, C.; Park, J. H.; Byun, D.; Lim, J. C.; Lee, J. K. Oxidation-resistant hybrid metal oxides/metal nanodots/silver nanowires for high performance flexible transparent heaters. *Nanoscale* **2016**, *8*, 3307–3313.

[17] Zhang, X.; Yan, X. B.; Chen, J. T.; Zhao, J. P. Large-size graphene microsheets as a protective layer for transparent conductive silver nanowire film heaters. *Carbon* **2014**, *69*, 437–443.

[18] Ji, S. L.; He, W. W.; Wang, K.; Ran, Y. X.; Ye, C. H. Thermal response of transparent silver nanowire/PEDOT:PSS film heaters. *Small* **2014**, *10*, 4951–4960.

[19] Chen, J. Y.; Chen, J.; Li, Y.; Zhou, W. X.; Feng, X. M.; Huang, Q. L.; Zheng, J. G.; Liu, R. Q.; Ma, Y. W.; Huang, W. Enhanced oxidation-resistant Cu-Ni core–shell nanowires: Controllable one-pot synthesis and solution processing to transparent flexible heaters. *Nanoscale* **2015**, *7*, 16874–16879.

[20] An, B. W.; Gwak, E.-J.; Kim, K.; Kim, Y.-C.; Jang, J.; Kim, J.-Y.; Park, J.-U. Stretchable, transparent electrodes as wearable heaters using nanotrough networks of metallic glasses with superior mechanical properties and thermal stability. *Nano Lett.* **2016**, *16*, 471–478.

[21] Stewart, I. E.; Rathmell, A. R.; Yan, L.; Ye, S. R.; Flowers, P. F.; You, W.; Wiley, B. J. Solution-processed copper-nickel nanowire anodes for organic solar cells. *Nanoscale* **2014**, *6*, 5980–5988.

[22] Zhang, D. Q.; Wang, R. R.; Wen, M. C.; Weng, D.; Cui, X.; Sun, J.; Li, H. X.; Lu, Y. F. Synthesis of ultralong copper nanowires for high-performance transparent electrodes. *J. Am. Chem. Soc.* **2012**, *134*, 14283–14286.

[23] Rathmell, A. R.; Bergin, S. M.; Hua, Y.-L.; Li, Z.-Y.; Wiley,

B. J. The growth mechanism of copper nanowires and their properties in flexible, transparent conducting films. *Adv. Mater.* **2010**, *22*, 3558–3563.

[24] Zhai, H. T.; Wang, R. R.; Wang, W. Q.; Wang, X.; Cheng, Y.; Shi, L. J.; Liu, Y. Q.; Sun, J. Novel fabrication of copper nanowire/cuprous oxidebased semiconductor-liquid junction solar cells. *Nano Res*. **2015**, *8*, 3205–3215.

[25] Wang, X.; Wang, R. R.; Shi, L. J.; Sun, J. Synthesis of metal/bimetal nanowires and their applications as flexible transparent electrodes. *Small* **2015**, *11*, 4737–4744.

[26] Song, J. Z.; Li, J. H.; Xu, J. Y.; Zeng, H. B. Superstable transparent conductive Cu@Cu_4Ni nanowire elastomer composites against oxidation, bending, stretching, and twisting for flexible and stretchable optoelectronics. *Nano Lett.* **2014**, *14*, 6298–6305.

[27] Luo, X. X.; Gelves, G. A.; Sundararaj, U.; Luo, J.-L. Silver-coated copper nanowires with improved anti-oxidation property as conductive fillers in low-density polyethylene. *Can. J. Chem. Eng.* **2013**, *91*, 630–637.

[28] Chen, Z. F.; Ye, S. R.; Stewart, I. E.; Wiley, B. J. Copper nanowire networks with transparent oxide shells that prevent oxidation without reducing transmittance. *ACS Nano* **2014**, *8*, 9673–9679.

[29] Deng, B.; Hsu, P.-C.; Chen, G. C.; Chandrashekar, B. N.; Liao, L.; Ayitimuda, Z.; Wu, J. X.; Guo, Y. F.; Lin, L.; Zhou, Y. et al. Roll-to-roll encapsulation of metal nanowires between graphene and plastic substrate for high-performance flexible transparent electrodes. *Nano Lett*. **2015**, *15*, 4206–4213.

[30] Ahn, Y.; Jeong, Y.; Lee, D.; Lee, Y. Copper nanowire–graphene core–shell nanostructure for highly stable transparent conducting electrodes. *ACS Nano* **2015**, *9*, 3125–3133.

[31] Shi, L. J.; Wang, R. R.; Zhai, H. T.; Liu, Y. Q.; Gao, L.; Sun, J. A long-term oxidation barrier for copper nanowires: Graphene says yes. *Phys. Chem. Chem. Phys.* **2015**, *17*, 4231–4236.

[32] Hong, S.; Lee, H.; Lee, J.; Kwon, J.; Han, S.; Suh, Y. D.; Cho, H.; Shin, J.; Yeo, J.; Ko, S. H. Highly stretchable and transparent metal nanowire heater for wearable electronics applications. *Adv. Mater.* **2015**, *27*, 4744–4751.

[33] Wang, R. R.; Zhai, H. T.; Wang, T.; Wang, X.; Cheng, Y.; Shi, L. J.; Sun, J. Plasma-induced nanowelding of a copper nanowire network and its application in transparent electrodes and stretchable conductors. *Nano Res.* **2016**, *9*, 2138–2148.

[34] Sellinger, A. T.; Wang, D. H.; Tan, L.-S.; Vaia, R. A. Electrothermal polymer nanocomposite actuators. *Adv. Mater.* **2010**, *22*, 3430–3435.

[35] Lee, S. M.; Lee, J. H.; Bak, S.; Lee, K.; Li, Y.; Lee, H. Hybrid windshield-glass heater for commercial vehicles fabricated via enhanced electrostatic interactions among a substrate, silver nanowires, and an over-coating layer. *Nano Res.* **2015**, *8*, 1882–1892.

[36] Choi, S.; Park, J.; Hyun, W.; Kim, J.; Kim, J.; Lee, Y. B.; Song, C.; Hwang, H. J.; Kim, J. H.; Hyeon, T. et al. Stretchable heater using ligand-exchanged silver nanowire nanocomposite for wearable articular thermotherapy. *ACS Nano* **2015**, *9*, 6626–6633.